

PACS numbers: 79.20.Eb; 81.07.–b
DOI: 10.1070/QE2015v045n08ABEH015681

Laser ablation of carbon targets placed in a liquid

A.A. Antipov, S.M. Arakelyan, S.V. Garnov, S.V. Kutrovskaya,
A.O. Kucherik, D.S. Nogtev, A.V. Osipov

Abstract. **We report experimental results on laser formation of carbon nanostructures produced during irradiation of a target placed in water. We have performed comparative experiments on laser heating of carbon targets by millisecond and femtosecond laser pulses. It is shown that under different conditions of laser irradiation of targets made of schungite, glassy carbon and pyrolytic graphite, different morphological types of micro- and nanostructured carbon are formed.**

Keywords: *laser ablation, carbon materials, nanostructures.*

1. Introduction

Investigation of processes of carbon modification under the action of laser radiation is an important direction of laser physics [1–5]. The use of laser radiation sources with different pulse durations allows one to change the rate of carbon heating, thereby realising various scenarios of the solid–liquid–vapour transition [6]. Recently, the methods of laser irradiation of carbon targets in a liquid medium have been actively developed [7]. In this case, depending on the irradiation conditions, it is possible to produce a cavitation bubble that can provide an additional pressure on a target surface with an amplitude of up to 10 GPa [7]. When use is made of femtosecond laser radiation, a transition of a liquid into a 'liquid plasma' state is possible near a target surface [8], which leads to both high temperature and high pressure in the irradiated region.

This paper describes experiments on laser irradiation of carbon targets placed into water. To implement various regimes of the target surface modification and formation of micro- and nanoparticles in a liquid we used two laser light sources – an Nd:YAG laser with a pulse duration of 0.2 ms (pulse energy up to 50 J) and a Ti:sapphire femtosecond laser with a pulse duration of ~50 fs (pulse energy up to 0.8 mJ).

2. Experimental conditions

In the experiments we used schungite, glassy carbon and pyrolytic graphite to prepare colloidal carbon systems that were employed as targets. The selected samples of carbon materials have different density, porosity and degree of graphitisation, which provides the development of various processes of particle modification and formation in a liquid during laser irradiation [9]. We used distilled water as a liquid medium. As shown in our works on deposition of carbon micro- and nanostructures by laser ablation in air [10], in the course of interaction free carbon atoms form bonds with oxygen and produce volatile compounds that do not affect the structure of the deposited layer. Therefore, during irradiation in water, one can expect similar effects.

The parameters of the laser radiation sources are listed in Table 1.

Selection of the laser sources is stipulated by the possibility of implementing various laser-induced processes [11–13]. Abramov et al. [11, 12] have shown that in using repetitive millisecond laser pulses, one observes melting of a carbon target. However, when a target is in a liquid, the resulting additional pressure can lead to implementation of new regimes of target surface modification after reaching equilibrium conditions. On the other hand, in using ultra-short laser pulses, one can obtain supercritical temperature and pressure [7]; however, these processes will occur in non-equilibrium conditions [6] and require a more detailed analysis. In the present study, laser irradiation was performed in the stationary regime and by scanning the target surface by a laser beam at a rate from 100 μm s^{-1} to 1 mm s^{-1}; the laser spot size on the target surface in different experiments was 50–200 μm.

Table 1. Parameters of the lasers.

Laser radiation	Laser	Laser wavelength/μm	Average pulse energy/J	Pulse duration/s	Pulse repetition rate/Hz	Beam quality M^2
quasi-cw	Nd:YAG	1.06	0.5–50	$(0.2–2)\times10^{-3}$	2–50	1.2
femtosecond	Ti:sapphire	0.8	$(0.1–0.8)\times10^{-3}$	$(5–10)\times10^{-14}$	100 (1000)	1.2

A.A. Antipov, S.M. Arakelyan, S.V. Kutrovskaya, A.O. Kucherik, D.S. Nogtev, A.V. Osipov Vladimir State University named after Alexander and Nikolay Stoletovs, ul. Gorkogo 87, 600000 Vladimir, Russia; e-mail: kucherik@vlsu.ru;
S.V. Garnov A.M. Prokhorov General Physics Institute, Russian Academy of Sciences, ul. Vavilova 38, 119991 Moscow, Russia

Received 25 September 2014; revision received 29 January 2015
Kvantovaya Elektronika **45** (8) 731–735 (2015)
Translated by I.A. Ulitkin

3. Results and discussion

The obtained results refer to two components of the system under study: the target itself and colloidal system that arises during laser ablation of a target placed in a liquid.

3.1. Morphology of the target surface after laser irradiation

After laser irradiation the target surface was examined by a Quanta 200 3D scanning electron microscope (SEM).

When the target surface (pyrolytic graphite) was exposed to 2-ms, 5-J laser pulses with a spot size of 50 μm on the target (stationary regime), we observed the formation of a complex domain structure (Fig. 1a), which differs substantially from the original structure of the pyrolytic graphite surface.

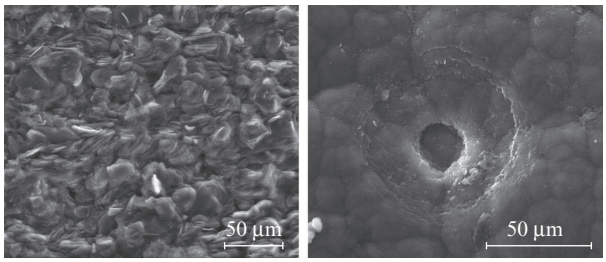

Figure 1. SEM images of the pyrolytic graphite surface after laser treatment by (a) millisecond and (b) femtosecond pulses.

During irradiation of the pyrolytic graphite target by 50-fs, 0.4-mJ femtosecond laser pulses with a spot size of 50 μm on the target, a cavity with a complex structure is formed (Fig. 1b). The external region consists of 'terraces' that gradually descend to a central dip forming an inner cavity area. It can be seen that the target material was unevenly removed; broken border lines allow us to speak of the destruction of the target due to the explosive mechanism of destruction in the pores.

For comparison, we present SEM images for targets made of glassy carbon and schungite after scanning the surface by a femtosecond laser pulse (Fig. 2). Schungite is a natural analogue of glassy carbon and has an amorphous structure; special interest in schungite is associated with the presence of fullerenes in its structure [14–16]. Porosity of schungite samples can reach 40% by volume [16], while a typical porosity value of glassy carbon is less than 1%.

In both cases, we observed the formation of chips and cracks, but on the surface of schungite (Fig. 2b) a system of caverns with a significant deviation of their boundaries from the scanning direction of the laser beam was formed.

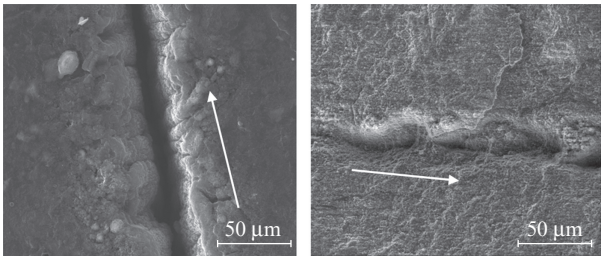

Figure 2. SEM images of (a) glassy carbon and (b) schungite target surfaces after scanning by femtosecond laser pulses at a rate of 100 mm s^{-1}. The arrows indicate the direction of scanning of the target surface.

3.2. Synthesis of colloidal systems under laser irradiation

In laser ablation of a target placed in a liquid, colloidal systems are formed, the key characteristics of which are the size of the synthesised nanoparticles and the function of their size distribution.

The morphological properties of the resulting particles. Under irradiation of a carbon target, nanoparticles and their clusters as well as sub-micron and micron particles are formed in the colloid volume. The process of their formation is governed by the regime of laser exposure and the target material (Table 2). The function of the particle size distribution was measured using an Horiba LB-550 dynamic light scattering particle size distribution analyser.

The smallest particles in the colloid were obtained for a glassy carbon target. Since its porosity is low, a traditional (ablation) scenario of the target material removal develops. For the schungite target the particles had a maximum size which can be attributed to a volume explosion in the pores.

The measured histograms of the particle size distribution in the resulting colloidal system are shown in Fig. 3. At moderate

Table 2. Sizes of the synthesised particles for different conditions.

Laser radiation	Intensity/ W cm^{-2}	Target material	Average size of synthesised particles in the colloid/nm
quasi-cw	10^6–10^8	glassy carbon	40–180
		pyrolytic graphite	130–540
		schungite	560–1320
femto-second	10^{13}–10^{15}	glassy carbon	120–370
		pyrolytic graphite	300–660
		schungite	3000–3700

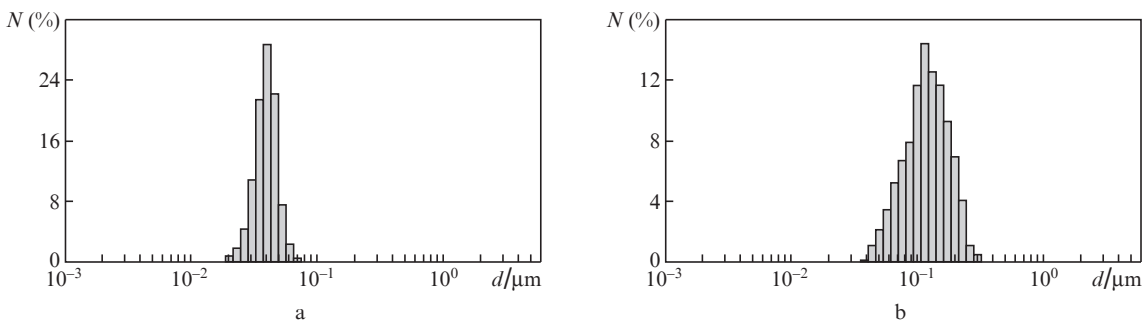

Figure 3. Histograms of the particle size distribution in the colloid after irradiation of the glassy carbon target in water by (a) quasi-cw laser pulses with an intensity $I = 10^6$ W cm^{-2} and by (b) ultrashort laser pulses with $I = 10^{13}$ W cm^{-2}.

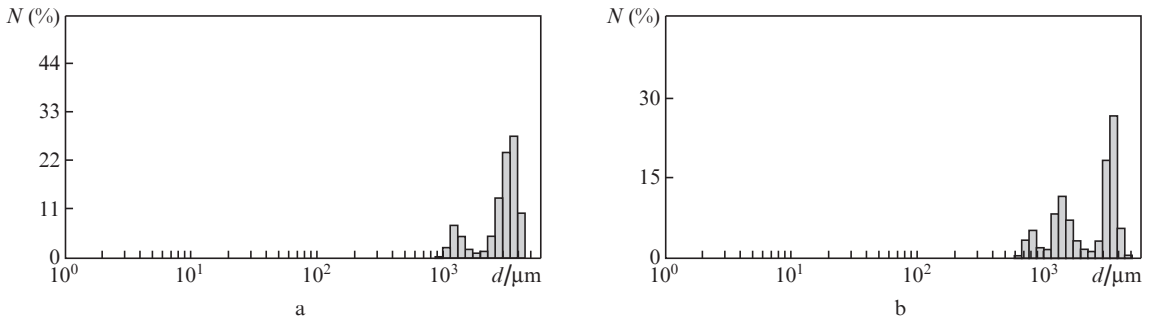

Figure 4. Histograms of the particle size distribution in the colloid after irradiation of the schungite target in water by 50-fs laser pulses with I = (a) 10^{13} and (b) 10^{15} W cm^{-2}.

laser intensities the distribution of nanoparticles is narrowly localised near their average size of 40 nm (Fig. 3a); under irradiation by femtosecond laser pulses there is a significant variance in the sizes of the resulting particles – their average size is about 100 nm (Fig. 3b).

Other results were obtained for the carbon particles synthesised during laser ablation of the schungite target: the histogram shows a bimodal particle size distribution (Fig. 4a), typical for high-intensity laser irradiation of the target [8].

We have also found that with increasing laser intensity the distribution of the particles changes from bimodal to trimodal (Fig. 4b), which is determined by various scenarios of the development of laser-induced processes. Firstly, at the initial instant of time there may develop a defect–deformation surface instability, leading to the formation of particles with a bimodal distribution in the colloidal systems [17]. Then, in using high-intensity laser pulses and in injecting additional pressure from the cavitation bubble, a melt can be formed whose droplets under the action of the recoil vapour pressure are also injected into the melt, which explains the appearance of the third peak in the histogram [18].

The presence of the third peak may also be associated with an increase in the absorption of radiation by particles of maximum (micron) size and, consequently, with a further fragmentation of the particles. These effects are determined by both selective absorption at the wavelength used (~800 nm) and by an overall increase in total absorption due to supercontinuum generation during the interaction femtosecond laser radiation with water [8].

To confirm this hypothesis, we calculated the absorption cross section (Fig. 5) for spherical particles (with diameters of 1–6 μm) of amorphous carbon using the Mie theory [19]. The data on the complex refractive index $\varepsilon = n + ik$ of amorphous carbon were taken for a laser wavelength of 800 nm [20]: $n = 1.9618$ and $k = 0.8061$.

The absorption cross section Q_{abs} was defined as the difference between the extinction cross section Q_{ext} and scattering cross section Q_{sca} [19]:

$$Q_{abs} = Q_{ext} - Q_{sca}, \tag{1}$$

where

$$Q_{ext} = \frac{2}{x^2}\sum_{m=1}^{M}[(2m+1)\,\mathrm{Re}(a_m + b_m)]; \tag{2}$$

$$Q_{sca} = \frac{2}{x^2}\sum_{m=1}^{M}[(2m+1)(|a_m|^2 + |b_m|^2)]; \tag{3}$$

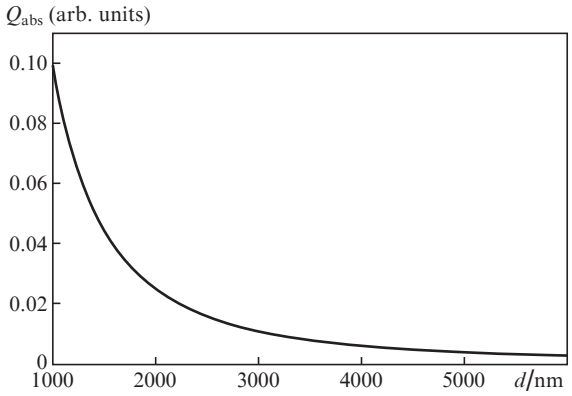

Figure 5. Dependence of the absorption cross section Q_{abs} on the particle diameter d.

$x = d\pi\varepsilon_2/\lambda_{vac}$; ε_2 is the dielectric constant of the medium; a_m and b_m are the Mie coefficients calculated for a given number m of partial waves in the interaction of laser light with a wavelength λ_{vac} with a particle of diameter d, for which n and k are defined above; and $M = x + 4x^{1/3}$ is the summation limit.

Then, we can determine the laser power absorbed by the particles of radius r:

$$P_{abs} = Q_{abs}\pi r^2 I_0, \tag{4}$$

where I_0 is the intensity of laser radiation. The absorbed power P_{abs} varies from ~10^7 W (for particles with a diameter 1 μm) to ~10^5 W (for particles with a diameter 6 μm) at the laser radiation intensity $I_0 \sim 10^{15}$ W cm^{-2}. It was sufficient for the effective fragmentation of nanoparticles.

Raman spectroscopy of colloidal systems. After laser irradiation of the targets placed in water, the resulting colloids were prepared by deposition-precipitation on a glass surface (Fig. 6) [21]. The structural features of these layers were studied by Raman spectra using an Ntegra Spectra probe nanolaboratory.

First of all it should be noted that even after high temperature treatment the structure of schungite samples usually has carbon globules or bulbous structures resistant to the thermal impact during heating up to temperatures 2700 °C [22]. The lack of such structures in our experiment during the deposition of particles from the colloids obtained by laser irradiation of a schungite target in water can be explained by the phase transformation of the target material. Meanwhile, for a glassy carbon target we observe mainly spherical particles

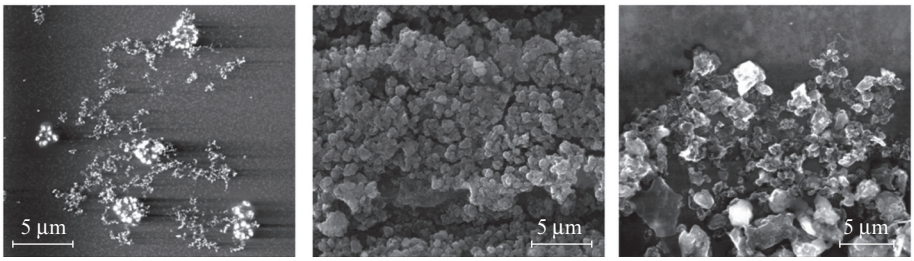

Figure 6. SEM images of (deposited on a glass substrate) structures from colloidal systems obtained for targets made of (a) glassy carbon, (b) pyrolytic graphite and (c) schungite after their irradiation in water by quasi-cw laser pulses with the intensity $I = 10^6$ W cm^{-2}.

in the deposited layer after they were deposited from the colloidal system onto the substrate.

All the spectra exhibit a quite intense band G located at $\nu = 1582$ cm^{-1} (Fig. 7). Thus, the obtained nano- and microstructures have carbon bonds with sp^2-hybridisation; broadening of peaks indicates the presence of different carbon–carbon bonds in the structure of the particles (this broadening is most noticeable under quasi-cw irradiation [16]).

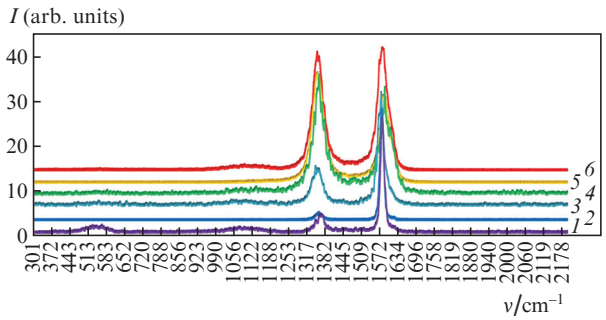

Figure 7. Raman spectra of the deposited carbon structures, obtained during irradiation of (*1*, *2*) pyrolytic graphite, (*3*, *4*) glassy carbon and (*5*, *6*) schungite targets by (*1*, *3*, *5*) millisecond and (*2*, *4*, *6*) femtosecond laser pulses duration.

The appearance of the band at $\nu = 1620$ cm^{-1}, as well as low-frequency branches of this band and the band D indicates the presence of carbon bonds with sp^3-hybridisation due to surface defects. This is explained by the formation of nanocrystalline diamond of different dimensions [23]. As a result, due to distortions of the lattice at the edge of these nanocrystals, additional bands appear in the Raman spectrum and the intensity of the main band of the detected spectrum decreases.

A broad band at $\nu = 520$ cm^{-1}, the most intense for a pyrolytic graphite target after exposure to quasi-cw laser radiation, corresponds to amorphous carbon with sp^3-hybridisation.

The bands in the range 1350–1580 cm^{-1} for schungite targets are typical for this material; the change in the intensity ratio of the peaks for the quasi-cw and femtosecond pulses allows us to speak about the structural transformations of the material, depending on the irradiation conditions; the shift of the band centre from 1600 cm^{-1} is associated with a decrease in the size of packs of graphene layers [16].

Thus, the experiments performed demonstrate the possibility of producing carbon micro- and nanostructures with varying degrees of graphitisation, depending both on the target material and on the conditions of laser irradiation.

4. Conclusions

We have presented the results of experiments on high-energy and high intensity laser irradiation of different carbon targets placed in water. Examination of the target surface after irradiation has shown the development of various laser-induced processes that depend on the laser pulse duration and the target material. We have shown the possibility of producing carbon nanoparticles with a histogram of the size distribution in which one can observe a small deviation of the particle size from the mean values during moderate-intensity irradiation of a target placed in water. We have demonstrated the change in the Raman spectra depending on the experimental conditions. Our results can be used to develop new physical principles of preparation of different nanostructured carbon materials with variable properties.

Acknowledgements. This work was partially supported within the framework of the State Research Task of Vladimir State University (Grant No. 2014/13) and by the RF President's Grants Council (State Support to Leading Scientific Schools Programme, Grant No. NSh-89.2014.2; and State Support to Young Scientists of Russia Programme, Grant No. MK-4321.2014.2).

References

1. Naumov V.G., Cherkovetch V.E., et al. *Proc. SPIE Int. Soc. Opt. Eng.*, **6344**, 63441N (2006), DOI:10.1117/12.694418.
2. Eliezer S., Eliaz N., et al. *Laser Part. Beams*, **23**, 15 (2005).
3. Shafeev G.A., Obraztsova E.D., Pimenov S.M. *Appl. Phys. A*, **65**, 29 (1997).
4. Riascos H., Neidhardt J., Radnoczi G.Z., et al. *Thin Solid Films*, №497, 1 (2006).
5. Gordienko V.M., D'yakov V.A., et al. *Kvantovaya Elektron.*, **37** (3), 285 (2007) [*Quantum Electron.*, **37** (3), 285 (2007)].
6. Asinovskii E.I., Kirillin A.V., Kostanovskii A.V. *Usp. Fiz. Nauk*, **172** (8), 931 (2002).
7. Wang C.X., Yang G.W. In: *Laser Ablation in Liquids: Principles and Applications in the Preparation of Nanomaterials* (Singapore: Pan Stanford Publishing, 2012) Ch. 3, pp 157–206.
8. Makarov G.N. *Usp. Fiz. Nauk*, **183** (7), 673 (2013).
9. Antipov A.A., Arakelyan S.M., et al. *Khim. Fiz. Mezoskop.*, **14** (3), 401 (2012).
10. Arakelyan S.M., Gerke M.N., Kutrovskaya S.V., Kucherik A.O., Prokoshev V.G. *Kvantovaya Elektron.*, **38** (1), 73 (2008) [*Quantum Electron.*, **38** (1), 73 (2008)].
11. Abramov D.V., Arakelian S.M., Galkin A.F., et al. *Pis'ma Zh. Eksp. Teor. Fiz.*, **84** (5), 315 (2006).
12. Abramov D.V., Arakelian S.M., et al. *Kvantovaya Elektron.*, **39** (4), 333 (2009) [*Quantum Electron.*, **39** (4), 333 (2009)].
13. Arakelian S., Zimin S., et al. *Laser Phys.*, **24**, 074010 (2014).
14. Buseck P.R., Tsipursky S.J., Hettich R. *Science*, **257**, 215 (1992).

15. Rozhkova N.N., Gribanov A.V., Khodorkovskii M.A. *Diamond Relat. Mater.*, **16**, 2104 (2007).
16. Golubev E.A. *Fiz. Tverd. Tela*, **55** (5), 995 (2013).
17. Emel'yanov V.I. In: *Laser Ablation in Liquids: Principles and Applications in Preparation of Nanomaterials* (Singapore: Pan Stanford Publishing, 2012) Ch. 1, pp 1–110.
18. Serkov A.A., Barmina E.V., Shafeev G.A., Voronov V.V. *Appl. Surf. Sci.*, **348**, 16 (2014); http://dx.doi.org/10.1016/j.apsusc.2014.12.139.
19. Bohren C.F., Hoffman D.R. *Absorption and Scattering of Light by Small Particles* (New York: Wiley, 1983; Moscow: Mir, 1986).
20. http://refractiveindex.info/?shelf=main&book=C&page=Hagemann.
21. Antipov A.A., Arakelyan S.M., et al. *Opt. Spektrosk*., **116** (2), 166 (2014).
22. Kholodkevich S.V., Berezkin V.I., Davydov V.Yu. *Fiz. Tverd. Tela*, **41** (8), 1412 (1999).
23. Baidakova M.V., Kukushkina Yu.A., Sitnikova A.A., et al. *Fiz. Tverd. Tela*, **55** (8), 1633 (2013).